# Cooperative processes during plastic deformation in nanocrystalline fcc metals: A molecular dynamics simulation

A. Hasnaoui, H. Van Swygenhoven, and P. M. Derlet
*Paul Scherrer Institute, Villigen, CH-5232, Switzerland*
(Received 2 July 2002; published 27 November 2002)

Large scale molecular dynamics (MD) simulations are used to simulate the plastic deformation of a nanocrystalline model Ni sample with an average grain size of 5 nm containing 125 grains at 800 K up to 4.0% plastic strain. For the first time in MD simulation, emerging shear planes involving several grain boundaries have been observed indicating cooperative plastic deformation activity between grains. It is found that three mechanisms have been involved in the development of such shear planes: grain-boundary migration, continuity of shear plane via intragranular slip, and rotation and coalescence of grains.

DOI: 10.1103/PhysRevB.66.184112 PACS number(s): 62.25.+g, 87.64.Aa, 61.72.Mm, 61.72.Bb

## I. INTRODUCTION

The potential for nanocrystalline (nc) materials (grain size $<100$ nm) to transform many technologies has been discussed recently in several works.[1–3] These materials exhibit unique microstructure[4,5] in which the number of atoms belonging to the grain-boundary (GB) region is significant, offering the possibility of physical properties which are unique to the nc regime. In particular, the mechanical properties of nc materials have received considerable attention in recent years.[6–11]

The deformation behavior of nc materials is characterized by features that are different from those of their coarse-grained counterparts. The nature of these deviations remains a subject of controversy. In general, two categories of theoretical models have been introduced to understand the origin of the phenomena discussed:[12] (i) Two-phase models that describe mechanical characteristics in nc materials as a weighted sum of the contributions of grain interiors and grain boundaries. These models do not explicitly take into account the evolution of defects and transformations of the grain boundary structure, and therefore cannot include possible emergent collective processes. (ii) Models describing plastic flow based on the evolution of defects and grain-boundary structure, through the description of physical mechanisms (lattice dislocation motion, grain-boundary sliding (GBS), and diffusion-limited plasticity mechanisms). These models involve the interaction and competition between various deformation mechanisms, each of which may have a nontrivial dependence on grain size, grain structure, and more generally atomic-scale structure.

The latter approach can thus admit the possibility of collective processes, an example of which being the formation of plane interfaces at a scale greater than the grain size, leading to long-range sliding. For instance, the model of Hahn *et al.*[6,7] suggests that grain-boundary sliding controls the deformation mechanism, and that, in order to overcome grain-boundary obstacles, two or more grain boundaries must cooperate to form a plane interface, which then by further interconnection with other plane interfaces, will lead to long-range sliding. In order to accommodate these plane interfaces, the local migration of GBs is necessary. Such migration involves a change in the triple junction (TJ) geometry and more generally TJ migration. The developing structures might be associated with shear planes, where high plastic deformation is localized, resulting in a larger macroscopic deformation of nc metals. Shear planes have been recently observed in nc material during deformation at low and high strain rates.[13,14] These are indications that cooperative processes are active in the nc regime.

From the perspective of superplasticity, several mechanisms leading to collective processes have already been studied (see Zelin and Mukherjee[15] and Mukherjee[16] for a review). It was suggested by Kaibyshev[17] that the micromechanism of cooperative grain-boundary sliding (CGBS) is a motion of grain-boundary dislocations (GBDs) along the adjacent interface of many grains and that this is stimulated by intragranular slip. Furthermore, CGBS has been suggested to be coupled with cooperative grain-boundary migration and cooperative grain rotation.[15,18] Zelin and Mukherjee[18] observed that after CGBS, grains can change their neighboring grains. They also suggested that the accommodation mechanisms, providing compatibility of the deformation in some grains, could be realized by migration of sliding GBs (to make the shear surface more planar), rotation of grains, intragranular deformation, and migration of GBs across the shear plane.

It has been observed experimentally that when two shear planes are operative, they might be active simultaneously or sequentially.[15] Rotation of grain groups in this case can be caused by the change in the orientation of CGBS planes, as well as accommodation deformation providing compatibility of strain of sliding grain groups.[15] Sheikh-Ali and Garmestani[19] suggested in their model that there are two components of GBS: so-called ''pure'' GBS that does not interact with intragranular slip and slip-induced GBS. The authors observed that in Zn-0.4%Al, the GBS in the presence of intragranular slip can be an order-of-magnitude faster than ''pure'' GBS. Baudelet[20] suggested that in grains, the location of which could not be accommodated with the local GB migration, continuity of a shear plane might be provided by intragranular slip. Experimentally Astanin *et al.*[21,22] have shown that in addition to local GB migration, the intragranular slip is a possible way of transmission of shear through a TJ.

 

Large-scale molecular dynamics (MD) simulations have proved to be a particularly useful tool for the atomic-scale study of structure and mechanical properties in nc materials.[23–29] By virtue of the nanometer grain-size scale, it is now possible to simulate atomistically, fully three-dimensional (3D) grain and GB networks, containing many grains. The physical time scale accessible to MD is, however, too short to obtain large deformations at strain rates typically realized in experiment. Thus superplasticity cannot be directly addressed. Nevertheless, past work has revealed, and elucidated on, plastic deformation processes such as GBS and dislocation nucleation at GBs, which may be considered as processes that play an important role in plasticity. Thus only the initial stages of large strain plasticity can be directly observed using MD,[30] which may include some form of collective motion such as that observed in superplastic deformation mechanisms. Indeed, experimental evidence of shear plane formation (and therefore cooperative GB sliding occurrence) in nc Ni at a low plastic deformation level (3%) is given by Dalla Torre *et al.*[13]

In the present work we report on the observation of collective processes using the MD simulation technique. The computer nc sample used has been especially designed to facilitate such an investigation. The sample contains 125 grains at a mean grain size of 5 nm, with no texture. The large number of grains are necessary in order to minimize the effects imposed by the periodicity used to simulate bulk conditions. The small grain size is chosen to reduce the total number of atoms in the sample (to 1.2 million) so that longer deformation times are possible at acceptable strain rates. Previous work has demonstrated that at room temperature, plastic deformation at these grain sizes is mainly accommodated in the grain boundary by means of atomic shuffling and stress-assisted free volume migration.[25] We therefore intentionally have chosen to perform the current simulation at 800 K to increase grain-boundary activity.

## II. SAMPLE PREPARATION AND SIMULATION TECHNIQUE

The sample used in the present work is constructed by beginning with an empty simulation cell with fully 3D periodic boundary conditions and choosing randomly 125 positions, such that the characteristic distance between them is 5 nm. The starting simulation cell has a side length of 68 Ni lattice constants. From each location, a fcc lattice of random orientation is geometrically constructed until there is an overlap between neighboring fcc lattice grains. Where there are nearest-neighbor distances of less than 2 Å, one atom is removed. This procedure produces a three-dimensional nc structure according to the Voronoi construction.[31] Molecular statics and MD at 300 K for 50 ps are then performed to relax and equilibrate the structure. The MD is performed using the Parrinello-Rahman Lagrangian[32] with orthorhombic simulation cell geometry conditions. We used the second moment tight-binding potential of Cleri and Rosato for ''model'' fcc Ni.[33] Thus the Ni sample of 1.2 million atoms contains 125 randomly oriented grains with all types of misfit from low angle to high angle grain boundaries. The relaxed structure has a final density of 97.8% of the perfect crystalline value. It contains 28.7% GB (non-fcc and non-hcp) atoms. The sample is then brought to a temperature of 800 K and a further 50 ps of MD is performed prior to deformation.

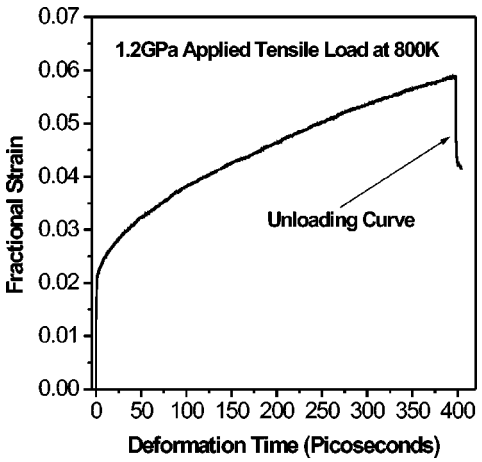


FIG. 1. The deformation curve of the 5-nm grain-size nc-Ni sample, under a uniaxial tensile load of 1.2 GPa performed at 800 K.

To analyze the grain boundaries we calculate the local crystalline order according to the Honeycutt analysis,[34] a technique based on determining the configuration of the common neighbors of a selected atom pair. For more details about this procedure applied in our simulations we refer to Ref. 24 Using this analyzing technique we defined four different classes of atoms to which different colors are attributed: gray represents fcc atoms, red represents first-nearest-neighbor hcp coordinated atoms, green represents other 12 coordinated atoms, and blue represents non-12 coordinated atoms. This tool has proved very helpful in the visualization of the grain-boundary structure and is helpful in identifying twin planes (one hcp {111} plane) and stacking faults (SF's) (two adjacent hcp {111} planes).[23–25] For black and white figures, light gray represents fcc atoms and black represents other atoms.

For this work, all atomic configurations and associated crystalline order analyses are derived from a 1ps average of the atomic spatial coordinates and the simulation cell size. Under load conditions, the 1ps averaging is performed under fixed simulation cell coordinates, that is, with the Parrinello-Rahman simulation cell control turned off. This was found to be necessary to eliminate the increased effects of thermal noise at 800 K. In this work, all deformation simulations are performed at 800 K under an applied uniaxial stress of 1.2 GPa, which is somewhat less than for the room-temperature simulations, and is done to reduce the strain rates to a reasonable value.

## III. RESULTS

### A. Statistical properties and mechanical behavior

Figure 1 displays the deformation curve obtained by MD simulation where the sample was deformed up to 400 ps

TABLE I. Statistics of different crystalline classes of atoms.

| | fcc atoms % of atoms | hcp atoms % of atoms | GB atoms % of atoms |
|---|---|---|---|
| As prepared | 68.89 | 2.44 | 28.67 |
| 2.2% deformed | 65.12 | 6.02 | 28.86 |
| 3.6% deformed | 62.83 | 8.61 | 28.56 |

resulting in a plastic strain of 4.0%. We have also unloaded the sample at 400 ps to estimate the elastic component to be about 1.5%. Inspection of this figure also revealed that the strain rate is about $7.2\times10^7$/s during the time spanning from 150 to 300 ps, reducing to $5.4\times10^7$/s after 350 ps. Such a reduction in strain rate over time is common in simulations of this type, and has been addressed in recent work by us.[35] In this work we will concentrate on three configurations from this deformation curve: the as-prepared one before loading, after 170 ps of deformation, which corresponds to 2.2% plastic deformation, and after 360 ps of deformation at 3.6% plastic deformation.

Table I shows the percentages of atoms according to their crystalline order where GB atoms correspond to non-fcc and non-hcp atoms. This differs from past work in that prior to this work, we have defined the GB atoms as non-fcc atoms. However as we shall see, this sample (even prior to loading) contains a non-negligible number of {111} hcp planes that pass through the edges of the 5-nm grains. Some hcp atoms are indeed located in the GB region and constitute important parts of the GB, however, this number is relatively low when compared to the number of GB atoms with ''other 12 coordinated'' and ''non-12 coordinated'' crystalline order, and thus does not significantly affect the GB atomic statistics. Table I clearly demonstrates that upon loading there is a net drop in the number of fcc atoms ($-3.77\%$ after 2.2% plastic deformation and a supplementary drop of $-2.29\%$ after 3.6% plastic deformation) accompanied by an increase in the number of hcp atoms (respectively, $+3.58\%$ and $+2.59\%$), whereas the number of GB atoms showed a slight variation not exceeding $\pm0.3\%$, indicating little change in the GB network. In conjunction with atomic visualization, this result shows, in contrast to room temperature deformation,[23–25,35] that although the grain size of our sample is very small (5 nm) we observe under deformation at 800 K some intragrain activity evidenced by the presence of stacking fault defect structures mainly at the edges of the grains, see Sec. IV.

Table II details the percentages for GB atoms according to their coordination number *Z*. The table shows that while the total number of GB atoms remains practically constant, these

TABLE II. Statistics of different coordinated atoms in the GB region.

| | $Z>12$ % of atoms | $Z=12$ % of atoms | $Z<12$ % of atoms |
|---|---|---|---|
| As prepared | 1.498 | 9.9548 | 17.220 |
| 2.2% deformed | 1.736 | 10.747 | 16.373 |
| 3.6% deformed | 1.824 | 10.979 | 15.760 |

atoms tend to increase their coordination number. In general for metallic systems, the GB region will attempt to minimize its number of broken bonds, there being a close linear relationship between the grain-boundary energy and the number of broken bonds.[36] By analyzing the atomic activity via the temporal evolution of average GB atomic coordination, our previous work[35] was found to be consistent with this view, leading, for example, to a tendency to preserve as much as possible the bulk 12-fold coordination. Note that this structural reordering effect is less during the last 190 ps of deformation.

More detailed investigations on numbers of atoms that changed from one crystalline order to another has shown that, during the first 170 ps, 25% of GB atoms have become fcc and a similar number of atoms (initially fcc) have become GB atoms. Such an exchange between these two crystallinity classes suggests that around 25% of GB atoms are involved in GB migration. This number decreased to 20% during the last 190 ps of deformation, suggesting that less GB migration is involved between 2.2% to 3.6% of plastic deformation. Moreover only 3% of this variation involves so-called ''perfect'' fcc atoms, that is, those atoms in an fcc enviroment up to at least the fourth-nearest-neighbor shell and thus those atoms initially in the grain interior. This contribution has also decreased for the 3.6% deformed sample to only 1.7%. This finding is compatible with the general result that there is a reduction in strain rate as the loading simulation proceeds.

### B. Cooperative processes

A typical example of formation of common shear planes during deformation is presented in Fig. 2. Figure 2(a) displays the atomic positions prior to deformation and Fig. 2(b) shows the atomic positions after 3.6% plastic deformation. The section of displayed atoms is approximately 1.2-nm thick along the viewing direction and the indicated tensile direction is that projected onto the plane of the figure.

Comparison of Figs. 2(a) and 2(b) demonstrates that after 3.6% plastic deformation this section of the sample underwent a reorganization of the GB regions resulting in an alignment of multiple GBs to form two common shear planes indicated by the large black arrows in Fig. 2(b). Indeed, GBs 85-108, 10-17, 10-117, and 8-117 underwent a migration to align, resulting in a change in the TJ geometry to enable the formation of shear plane 1. The nature of the atomic activity that facilitates such migration is predominantly of the form of atomic shuffling with some stress-assisted free volume migration resulting in an increase in GB structural order similar to what we have seen in past works.[35,25] The orientation of shear plane 1 is inclined at about 53° to the tensile axis, whereas, shear plane 2 is orientated at 46° to the tensile axis, which is close to the maximum resolved applied shear at 45°.

Inspecting the region of Fig. 2, we observed that some grains move collectively relatively to some others. Arrows in Fig. 2(b) represent the relative sliding of some grains involved in this collective motion. The directions of the three nearly vertical arrows in Fig. 2(b) for shear plane 1 are de-

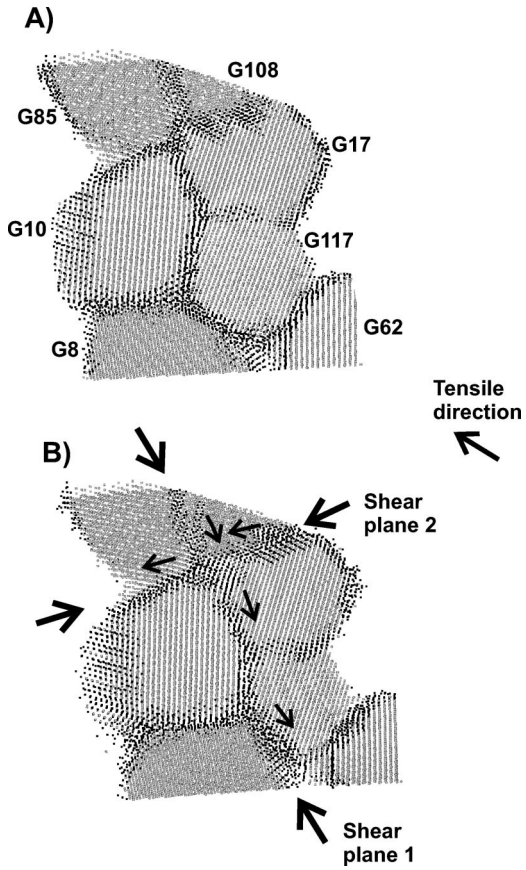


FIG. 2. A region of the nc-Ni sample, in which two shear planes (1 and 2) have been identified as indicated via the large arrows. The small arrows display the direction of the relative sliding between grains. (A) is the atomic configuration before loading, and (B) after 3.6% plastic deformation.

rived by the displacement of atoms in grains 108, 17, and 117 relative to the center of mass of the respective grains 85, 10, and 8. The length of arrows does not represent the absolute amount of sliding, which for all grains was typically between 1.5 and 2 Å. From this we see clearly that for shear plane 1, the group of grains (108, 17, and 117) slides relative to the second group of grains (85, 10, and 8). Much of this activity occurred during the first 2.2% of plastic deformation during which the shear interface was not completely formed. In addition to sliding, some grain rotation was observed, in particular, grain 8, which rotates approximately 1°. For shear plane 2, collective sliding of grains 85 and 108, relative to grains 10 and 17, respectively, was observed as indicated by the nearly horizontal arrows in Fig. 2(b). This activity occurred during the time separating the 2.2% and 3.6% plastic deformation, and thus predominantly after the activity associated with shear plane 1. Such sequential activity of shear interfaces has also been observed experimentally.[15,18]

Figure 3 now shows a close-up view of the triple junction region between grains 10, 17, and 117 in a different orientation to that of Fig. 2. In Fig. 3(a) atomic positions corresponding to the sample prior to deformation are drawn together with their atomic displacement (red lines) after 2.2% deformation. The atomic displacements are calculated relative to the center of mass of grain 10. Note that the sliding direction of grain 17 is the same as that represented in Fig. 2(a). As already mentioned, the atomic activity within the GB consists mainly of atomic shuffling with a small amount of short-range stress assisted free volume migration. This is in part evidenced in Fig. 3(a) by the larger atomic displacement vectors within the GB region.

In Fig. 3 we have marked by yellow, regions of misfit in GB 10-17. Although for this GB no coherency was observed between families of $\{111\}$ planes in both grains, an aligning of $\{111\}$ planes in grain 10 with $\{100\}$ planes in grain 17 was seen with misfit regions to accommodate the lattice mismatch between the two sets of planes. The atomic positions corresponding to 2.2% plastic deformation are shown in Fig. 3(b) with the corresponding regions of misfit marked again in yellow. We see that Figs. 3(a) and 3(b) show clearly that the misfit regions undergo a propagation to the left towards TJ 10-17-117. In addition we observe GB 10-17 migrating during this time in a direction towards grain 17. Along this section of displayed atomic positions, we also see that GB 10-17 shortens due to corresponding TJ 10-17-85 migration. The atomic positions corresponding to 3.6% plastic deformation are shown in Fig. 3(c) showing further propagation of one misfit region and the annihilation of the other at TJ 10-17-117, during the time separating the 2.2% and 3.6% plastic deformation configurations.

Figure 4 shows another section of the sample containing a different shear plane which we refer as shear plane 3. In this figure only non-fcc atoms are drawn and the color scheme used is that stated in Sec. II. The tensile axis is pointing down the page. Shear plane 3 is marked in yellow in Fig. 4(b). In Fig. 4(a) we draw the non-fcc atoms of the sample prior to deformation and indicate GB 41-105. This is a low angle GB consisting of a GBD network that dissociates into lattice Shockley partials. Figure 4(b) is the atomic configuration after 3.6% plastic deformation, and it can be seen that the creation of shear plane 3 involves the coalescence of grains 41 and 105. Detailed temporal analysis indicated that this coalescence occurred with significant GB migration that resulted in the shrinking of some grains on the right side of shear plane 3. This can be seen in Fig. 4(b). Shear plane 3 makes an angle of about 30° with the tensile axis.

A close-up view of the GB between grains 41 and 105 along a common $\langle 110 \rangle$ direction is presented in Fig. 5. In Fig. 5(a) the unit cells of both grains are highlighted in yellow and the crystallographic orientation of grain 41 is given. This GB is along a $(\bar{1}1\bar{1})$ plane of grain 41 and has a tilt angle of about 8° around a [110] axis with almost no twist character (less that 2°). In this view one can observe easily the two Shockley partials constituting the GB 41-105. The two leading partials of the partial dislocations have a Burgers' vector along $\langle 121 \rangle$ and $\langle 21\bar{1} \rangle$ directions with magnitudes of $0.91a_0/\sqrt{6}$ and $1.03a_0/\sqrt{6}$, respectively, where $a_0$ is the lattice parameter of bulk Ni. After 2.2% plastic deformation [Fig. 5(b)] we observe clearly that the two partial dislocations have propagated to an opposite GB region leaving behind a defect-free fcc region. This propagation is accompanied by a rotation of grain 105 resulting in a misori-

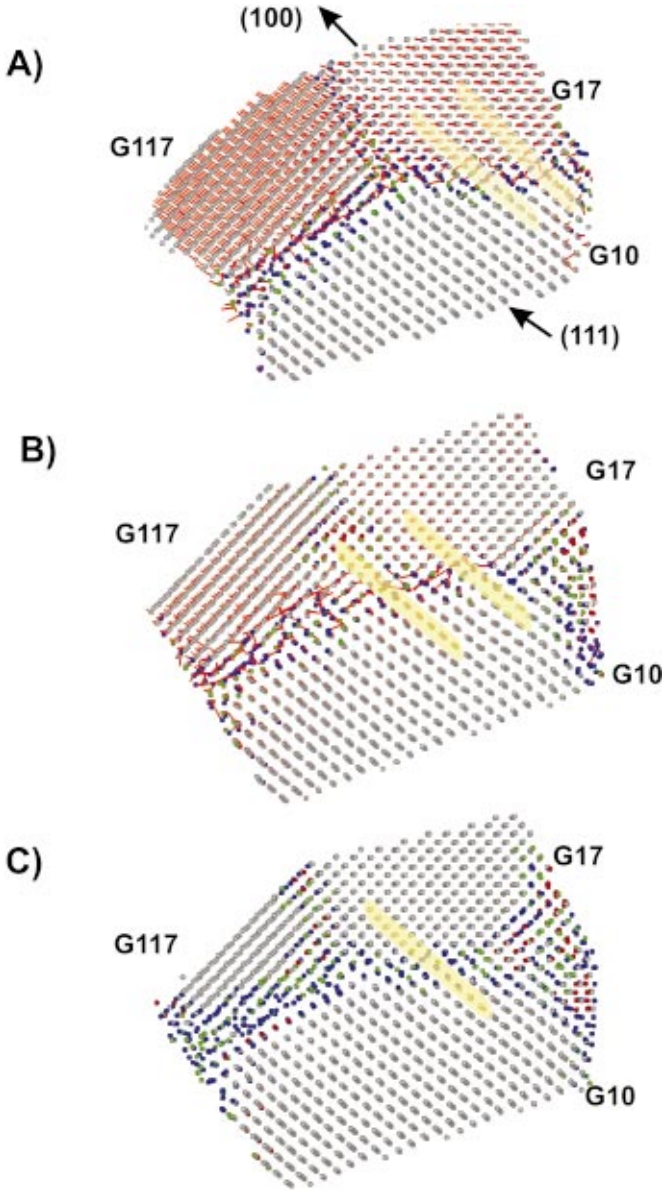


FIG. 3. (Color) Close up of atomic activity (red lines) in shear plane 1 (of Fig. 2). (A) is the atomic configration prior to loading, (B) is at 2.2% plastic deformation, and (C) is at 3.6% plastic deformation. The shaded yellow regions indicate regions of misfit between grains 17 and 10.

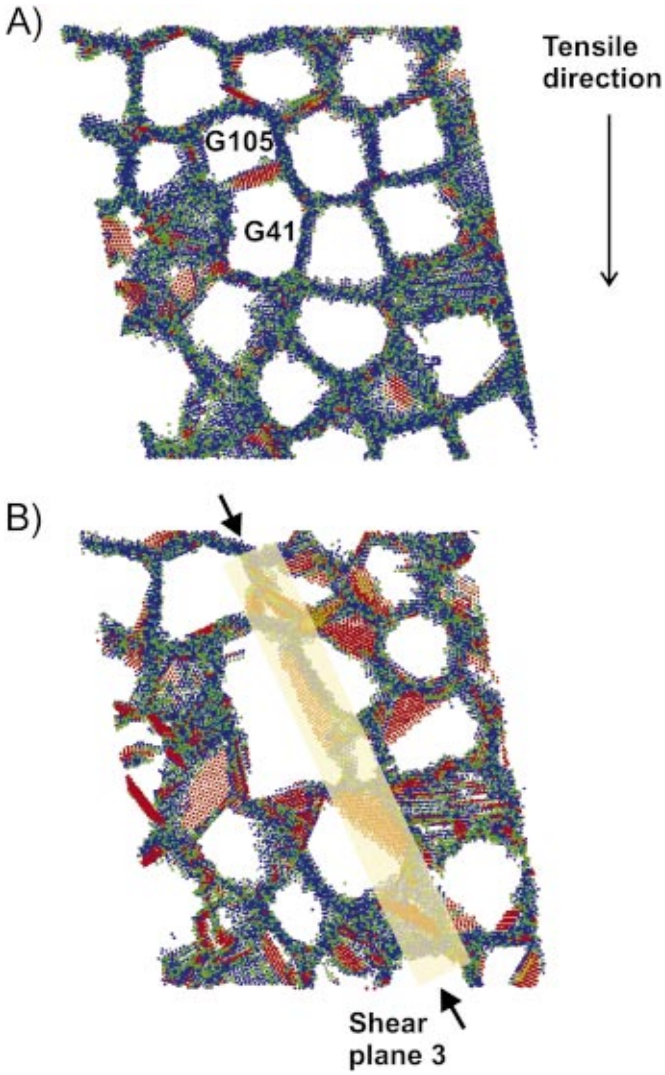


FIG. 4. (Color) A region of the nc-Ni sample, in which shear plane 3 has been identified as indicated via the shaded yellow region, where (A) is the atomic configuration before loading, and (B) after 3.6% plastic deformation. Coalescence of grains 105 and 41 is clearly evident.

entation between the two grains now of only 3°. By 3.6% plastic deformation, Fig. 5(b), both leading and trailing partial dislocations of each GBD have been absorbed by the GB region (between grains 105 and 23) resulting in a complete annihilation of the GB between grains 41 and 105, and thus their coalescence into one grain, the GB of which forms part of shear plane 3 indicated by the yellow shaded region in Fig. 4(b).

Figure 6 shows another region of the sample where a different shear plane has been identified, which we refer to as shear plane 4. Figures 6(a) and 6(b) represent, respectively, the atomic configurations prior to deformation and at 2.2% plastic deformation. After 2.2% plastic deformation a partial dislocation nucleates and propagates through grain 38 connecting GBs 50-55 and 53-88 to form shear plane 4. This can be seen by the red hcp stacking fault defect in Fig. 6(b). Thus in this case continuity of shear plane 4, indicated by the shaded yellow region in Fig. 6(b), is provided by intragranular slip in grain 38, the location of which could not be accommodated with the local GB migration. Such activity has been observed experimentally in microcrystalline materials (see Ref. 21, 22, and 17). The atomic displacements in this section of the sample showed that after 2.2% plastic deformation, grains 50, 38a (top subgrain of grain 38), and 53 slide to the right, relative to the centers of mass of grains 55, 38b (bottom subgrain of grain 38), and 88, respectively. We also observed a slight rotation (less than 2°) for grains 55, 88, and 53, which helps accommodate this process. After 3.6% plastic deformation (not shown) we didn't observe a notable change at the nc structure level. However, the sliding direction has changed and during the time separating the two levels of deformation we observed that grains 38a and 38b

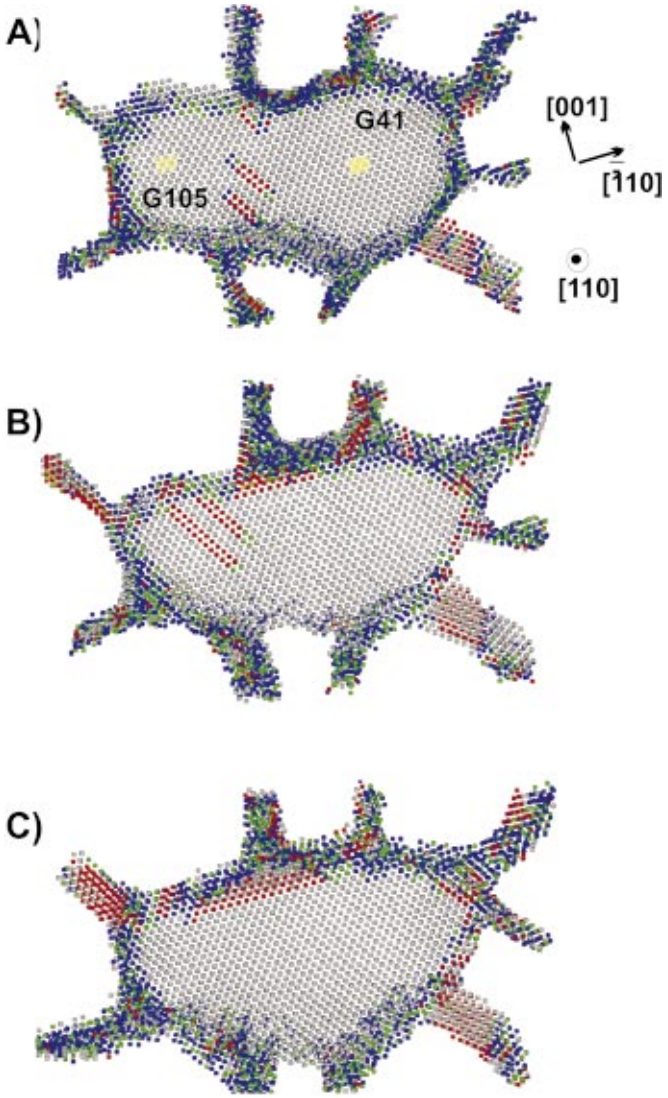


FIG. 5. (Color) Close-up view of partial dislocation activity in grains 105 and 41. (A) is the atomic configuration prior to loading, (B) is at 2.2% plastic deformation, and (C) is at 3.6% plastic deformation. The low angle GB 105-41 consists of disassociated Shockley partials, that upon loading propagate to the left to accommodate the coalescence of grains 104 and 41.

slide to the top of the page relative to grains 50 and 55 suggesting that the GBs 50-38 and 55-38 act as another shear plane in this region indicated by vertical arrows in Fig. 6(b) (shear plane 5), becoming operative after shear plane 4 has been activated in the earlier stages of deformation.

## IV. DISCUSSION

Previous work has shown that for the sub-20-nm grain-size regime, the dominant plastic deformation mechanism is GBS via atomic shuffling and free volume migration, and more recent work has demonstrated that such GBS is intimately related to GB and TJ migration, the nucleation of partial dislocations from the GB and an associated reorganization of the GB structure from the perspective of GB dislocation networks.[37] The dislocation nucleation process has

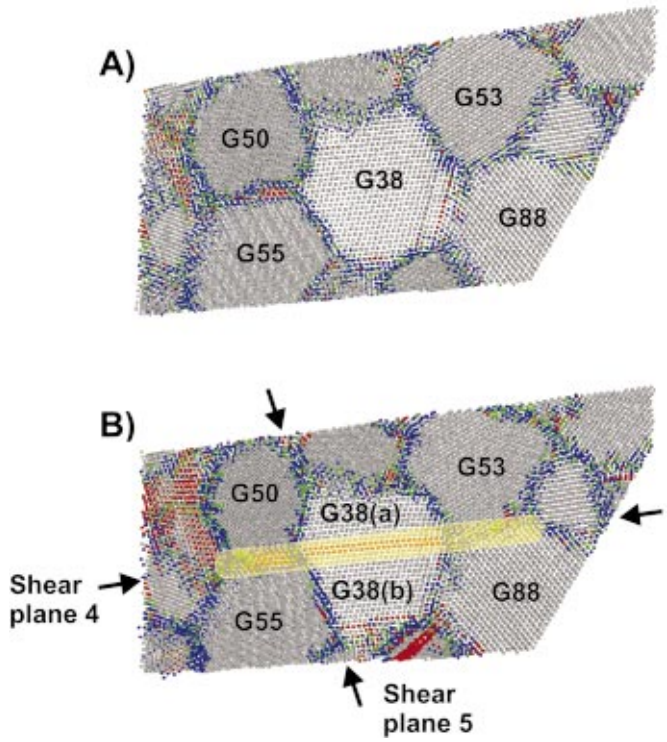


FIG. 6. (Color) A region of the nc-Ni sample, in which shear plane 4 has been identified as indicated via the shaded yellow region, where (A) is the atomic configuration before loading, and (B) after 2.2% plastic deformation. This is an example of where the continuity of a shear plane is provided for by intragranular slip in grain 38.

been found also to be intimately linked to atomic shuffling and free volume migration in the GB.

In the present work, we have also observed such phenomena during the deformation of a 125-grain 5-nm grain-size sample, resulting in the emergent process of collective grain motion via the formation of shear planes that extend over a number of grain sizes. These shear planes are all inclined to the tensile axis at angles ranging between 30° and 60°. A temporal analysis of atomic configurations as a function of deformation has also shown that these shear planes became active sequentially over the 400 ps of deformation performed. Thus, as has been experimentally seen in conventional grain-size materials,[21] CGBS processes in nc materials are possible even at deformations significantly less than that associated with superplasticity.

The observed underlying mechanisms taking part in the formation of these shear planes fall into three classes:

(i) GBS-induced migration of parallel and perpendicular to the developing shear plane GBs, to form a single shear plane consisting of a number of collinear GBs.

(ii) The coalescence of neighboring grains that have an initially low angle GB described by an array of disassociated Shockley partials, where presently, the coalescence was facilitated by the propagation of the partials to a nearby GB and subsequent reorientation of both grains into one crystallographic orientation.

(iii) Continuity of the shear plane by intragranular slip,

where presently a partial nucleated and propagated from one TJ of the developing shear plane to another.

In general the formation of a shear plane will involve all three mechanisms, it is, however, important to note that for the latter two classes accommodation of dislocation activity and coalescence will provide an additional driving force for subsequent GB migration along the lines of class 1. This is indeed what has been observed in the present work. This is also supported by results of Tables I and II where 25% of GB atoms are shown to be involved in GB migration. Class 2 may be considered in part a special consequence of grain rotation. Indeed grain rotation has been seen in the vicinity of other shear planes in the sample. Often rotation was accompanied with partial dislocation activity in and near the grain-boundary region of those grains involved.

Inspection of Fig. 4 reveals that a significant number of {111} hcp planes are formed during deformation. This is also reflected in Table I, where the percentage of hcp atoms rises from 2.44% to 6.02% at 2.2% plastic deformation, and to 8.61% at 3.6% plastic deformation. Inspection of the atomic configurations during deformation revealed that this increase arises from the formation of SFs. This is at variance to the previous deformation simulations for this grain size performed at 300 K,[23–25,35] where all plastic deformation is intergranular via GBS. An important observation concerning the nature of the SF presence at 800 K is that in most cases, the SFs are confined to the edges of the grains. Those examples where partial dislocations were seen to propagate into the interior of the grain could be identified as intragranular slip contributing to the formation and development of shear planes (class 3). A possible reason for increased presence of SFs at 800 K, when compared to 300 K deformation simulations, may in part lie in the associated reduction of the SF surface energy with increasing temperature. For the Ni potential used presently, we calculated the stacking fault energy density as a function of temperature and display this in Table III. We note that the calculated values decrease linearly with temperature. Thus the stacking fault energy decreases significantly at 800 K. In addition to this, general increased atomic activity in the GB may play an important role in the emission and propagation of partial dislocation, since in recent work it has been established that partial dislocation nucleation is intimately linked to grain-boundary activity, and partial dislocation core propagation,[37] which is pinned to neighboring GB regions, is coincident with GB structural reorganization.[38]

TABLE III. Ni stacking fault energies for Cleri and Rosato (Ref. 33) as a function of temperature. Those values given in parentheses are taken from Ref. 39.

| Temperature (K) | Stacking fault energy ($mJ/m^2$) |
|---|---|
| 0 | 304.8 (304.8) |
| 300 | 262.5 (262.4) |
| 800 | 195.5 |

## V. CONCLUSIONS

In conclusion the present work supports the picture presented by the model of Hahn *et al.*,[6,7] in which the dominant mechanism of plastic deformation via collective grain activity is that of grain-boundary sliding, and it is only at the nanoscale that the concurrent grain-boundary migration is enough to reduce the so-called steric hinderance of grains. Our work, however, suggests that it is not only the grain-boundary sliding mechanism, but also granular rotation and deformation via intergranular slip, which contribute to collective grain activity. With the limited number of grains and a deformation time of 400 ps, it is not yet possible to gain a quantitative contribution of each shear plane formation class. However it remains clear that a combination of grain-boundary migration via grain-boundary sliding and grain-boundary migration via intragranular slip and grain rotation is the dominant process by which shear planes form, and that collective grain-boundary sliding becomes an increasingly important plastic deformation mechanism at the 5-nm grain-size nc regime.

## ACKNOWLEDGMENTS

This work was supported by the Swiss NSF (Grant No. 2000-056835.99).

[1] A. S. Edelstain and R. C. Amarata, *Nanomaterials: Synthesis, Properties and Applications* (Institute of Physics, University of Reading, Berkshire, 1996).
[2] R. Siegel, E. Hwu, and M. Roco, *Research and Development Status and Trends in Nanoparticles, Nanostructured Materials, and Nanodevices in the United States* (International Technology Research Institute, Baltimore, 1997).
[3] N. Ledentsov, V. Ustinov, V. A. Shchukin, P. S. Kop'ev, Z. Alferov, and D. Bimberg, Semiconductors **32**, 343 (1998).
[4] H. Gleiter, Acta Mater. **48**, 1 (2000).
[5] C. Suryanarayana, Int. Mater. Rev. **40**, 41 (1995).
[6] H. Hahn and K. A. Padmanabhan, Philos. Mag. B **76**, 559 (1997).
[7] H. Hahn, P. Mondal, and K. A. Padmanabhan, Nanostruct. Mater. **9**, 603 (1997).
[8] N. Wang, Z. Wang, K. T. Aust, and U. Erb, Acta Metall. Mater. **43**, 516 (1995).
[9] R. S. Mishra and A. K. Mukherjee, Nanostruct. Mater. **9**, 473 (1997).
[10] R. S. Mishra, R. Z. Valiev, S. X. McFadden, and A. K. Mukherjee, Mater. Sci. Eng., A **252**, 174 (1998).
[11] R. Z. Valiev, Mater. Sci. Eng., A **234-236**, 59 (1997).
[12] M. Y. Gutkin, I. A. Ovid'ko, and C. S. Pande, Rev. Adv. Mater. Sci. **2**, 80 (2001).
[13] F. Dalla Torre, H. Van Swygenhoven, and M. Victoria, Acta Mater. **50**, 3957 (2002).
[14] E. Ma, Powder Metall. **43**, 306 (2000).
[15] M. G. Zelin and A. K. Mukherjee, Mater. Sci. Eng., A **208**, 210 (1996).

[16] A. K. Mukherjee, Mater. Sci. Eng., A **322**, 1 (2002).
[17] O. A. Kaibyshev, Mater. Sci. Forum **304-306**, 21 (1999).
[18] M. G. Zelin and A. K. Mukherjee, Acta Mater. **43**, 2359 (1995).
[19] A. D. Sheikh-Ali and H. Garmestani, Mater. Sci. Forum **357-359**, 393 (2001).
[20] B. Baudelet, Scr. Metall. Mater. **27**, 745 (1992).
[21] V. V. Astanin and O. A. Kaibyshev, Mater. Sci. Forum **170-172**, 23 (1994).
[22] V. V. Astanin, O. A. Kaibyshev, and A. I. Pshenichnyuk, Mater. Sci. Forum **243-245**, 41 (1997).
[23] H. Van Swygenhoven, M. Spacer, and A. Caro, Acta Mater. **47**, 3117 (1999).
[24] H. Van Swygenhoven, D. Farkas, and A. Caro, Phys. Rev. B **62**, 831 (2000).
[25] H. Van Swygenhoven and P. M. Derlet, Phys. Rev. B **64**, 224105 (2001).
[26] P. Keblinski, D. Wolf, S. R. Phillpot, and H. Gleiter, Scr. Mater. **41**, 631 (1999).
[27] V. Yamakov, D. Wolf, M. Salazar, S. R. Phillpot, and H. Gleiter, Acta Mater. **49**, 2713 (2001).
[28] H. Van Swygenhoven and A. Caro, Phys. Rev. B **58**, 11 246 (1998).
[29] V. Yamakov, D. Wolf, S. R. Phillpot, and H. Gleiter, Acta Mater. **50**, 61 (2002).
[30] H. Van Swygenhoven, Science **296**, 66 (2002).
[31] G. Z. Voronoi, J. Reine Angew. Math. **134**, 199 (1908).
[32] M. Parrinello and A. Rahman, J. Appl. Phys. **52**, 7182 (1981).
[33] F. Cleri and V. Rosato, Phys. Rev. B **48**, 22 (1993).
[34] J. D. Honeycutt and H. C. Andersen, J. Phys. Chem. **91**, 4950 (1987).
[35] A. Hasnaoui, H. Van Swygenhoven, and P. M. Derlet, Acta Mater. **50**, 3927 (2002).
[36] K. L. Merkle and D. Wolf, Mater. Res. Soc. Symp. Proc. **229**, 185 (1991).
[37] H. Van Swygenhoven, P. M. Derlet, and A. Hasnaoui, Phys. Rev. B **66**, 024101 (2002).
[38] P. M. Derlet and H. Van Swygenhoven, Scr. Mater. **47**, 719 (2002).
[39] R. Meyer and L. J. Lewis, Phys. Rev. B **66**, 052106 (2002).